RMS/EMT Simulation of Maesariang Microgrid System when Change Operation Mode

Chaiyaporn Kaewvata[1], Chatchai Sirisamphanwong[2,3,*], Tawat Suriwong[1,3]

[1]School of Renewable Energy and Smart Grid Technology, Naresuan University, Phitsanulok 65000, Thailand
[2]Smart Energy System Integration Research Unit, Department of Physics, Faculty of Sciences, Naresuan University, Phitsanulok 65000, Thailand
[3]Research Center for Academic Excellence in Applied Physics, Faculty of Science, Naresuan University, Phitsanulok 65000, Thailand
***Corresponding author's email:** chatchaisi@nu.ac.th
Received: 31/01/2021, Accepted: 06/03/2021

Abstract

This study cation demonstrates the performance of Maesariang Microgrid System (MMGS) during changing operation mode from grid connection to island in 2 cases and from island to grid connection in 2 cases. Stability Analysis (RMS) and Electromagnetic Transient (EMT) simulation by using DigSILENT Power Factory software is used to evaluate MMGS performance during switching the operation mode between grid connection mode and island mode that is the critical period of MMGS for controlling the network security, stability, reliability, and power quality of its service area. The behavior of active power generation from the PV system, the active and reactive power generation, voltage, and frequency from Battery Energy Storage System (BESS) at Maesariang substation in 50 s of the changing mode periods with and without communication time delay is studied for indicating MMGS performance in each simulation case. The simulation result presents that MMGS has impressive performance to manage all studied electrical parameter during changing mode from island to grid connection in all case and grid connection to island in the case that the spare generation power of BESS is higher than the lose incoming power and communication time delay has the unimportant effect to MMGS performance. In the contrary, MMGS performance during changing mode from grid connection to island in the case that the spare generation power of BESS is equal or lower than the lose incoming power is quite terrible and communication time delay are the precious factor to arbitrate the continuously operation or blackout in MMGS.

Keywords:

RMS, EMT, Simulation, Microgrid, Changing operation mode, Security, Stability, DigSILENT Power Factory

1. Introduction

Since 2000, Thailand power demand has been continuously increasing at about 4.22% per year [1]. The main factors driving the demand is population expansion and economic growth, However, new fossil-fueled centralized power plants to satisfy the rising demand has increasingly being constrained by the growing concerns on the environmental and social impacts, that include greater public opposition to these power plants. The development of renewable energy power plants is a key solution to increasing power generation capacities that avoid environmental and social problems. In Thailand, solar and wind are the main sources of renewable energy for electricity generation. The country currently has 3.5 GW solar, and 1.5 GW wind power installed capacities [2, 3].

However, electricity supply from these power systems can be unstable. There can be fluctuation in power production and that can result in power outages. The addition of solar and wind power plants in a Low Voltage Distribution System (LVDS) can cause of harmonics distortion, voltage and power fluctuation, frequency variations, and power factor [4-9]. Such power outages negatively impact the

economy and pose security problems in some areas. If these problems cannot be solved, supplying power from solar and wind systems to the grid can be difficult and unfeasible.

Microgrid systems can effectively deal with these problems. Microgrid systems are adaptable, allow for expandable and flexible sizing, and can apply intelligent or smart grid devices for power management. Microgrid systems can increased the affordability of renewable energy based Distributed Energy Resources (DERs). A microgrid system is an independent electrical network consisting of distributed loads, DERs, and energy storage, which can be controlled as a single power system. Normally, a microgrid is connected to a national grid. But the microgrid can also disconnect from the national grid and operate on "island mode". It can function autonomously and depends on commands based on site-specific physical and/or economic conditions distinct from those conditions for the main grid.

Microgrid systems have been implemented in many countries such as in the USA, in many European countries, in Japan, China, South Korea, and in Thailand. Microgrid systems were implemented to improve network security, stability, reliability, and the power quality in the regional area where the microgrid system is supplying electricity,

In Thailand, the School of Renewable Energy & Smart Grid Technology, Naresuan University (Sgtech-NU), in Phitsanulok province, has been demonstrating and operating the country's first PV-powered microgrid system since 2008 [10,11]. Since then, many organizations, particularly the government energy agencies such as Electricity Generating Authority of Thailand (EGAT), Metropolitan Electricity Authority (MEA), Provincial Electricity Authority (PEA), Energy Policy and Planning Office (EPPO), and including private organizations and companies, have also been conducting research, development, and implementation of microgrid systems. Many of these microgrid systems have increasing share of solar and wind energy generation [12-17].

2. Statement of the Study

2.1. Background

The Maesariang district in Mae Hong Sorn province is one of the weakest power network areas under PEA service. This area receives power from the Hot substation that is about 110 kilometers away from the district, using a 22 kV distribution line that passes through forest and backcountry areas. Therefore, the power network in this area has faced many problems due to the long distribution line such as, energy losses (about 19 % or 6.7 GWh/year), voltage sag, and power interruptions that lead to power outage of over 20 times per year. In addition, the feeder voltage from the grid-connected solar farm in this area, usually rises over the PEA upper limit when the power generation is high, and the load consumption is low. This result to the disconnection of the PV power plant from the distribution system and the loss of the power generation from the plant.

Because of these reasons, PEA decided to implement improvements in the Maesariang Microgrid system (MMGS) located in this district to solve these problems, and to improve the network security, stability, reliability, and power quality in the MMGS service area. The operation to change the operation of the MMGS from a grid connected mode to an island mode is a critical period for controlling the network security, stability, reliability, and power quality in the regional power area covered by the grid. Therefore, it is really a challenge to study the performance of MMGS during the switching operation mode.

2.2. Objectives and Expected Results

This paper aimed to present four simulation scenarios or cases of Stability Analysis (RMS) and Electromagnetic Transient (EMT) simulations of the MMGS using the DigSILENT Power Factory software, during the shifting of the operation of the microgrid system from a grid connected mode to an island mode. The simulations were performed using actual distribution network data and conducting actual technical assessment of the MMGS.

The simulation results should give indications on the impact on the network security, stability, reliability, and power quality of MMGS during the switching of the operation mode of the microgrid. Moreover, controlling techniques to increase the performance of the MMGS, and to decrease the impacts during changing of the operation mode, are expected to be developed also from the simulation results.

3. Case Study of the Maesariang Microgrid System

3.1. Maesariang Microgrid System (MMGS)

The MMGS started operation in the fourth quarter of 2020. The MMGS was constructed to improve the existing 22 kV Maesariang distribution system. New microgrid components were installed to upgrade the distribution system, such as a microgrid controller, a battery storage, a diesel generator, and a communication system.

The components of the MMGS include a 600 kW hydro generator system (HG), 4 MW diesel generator (DG), 4 MW PV system, 3 MW/1.5 MWh Battery Energy Storage System (BESS), the Microgrid controller, the communication system, and the Maesariang load (peak load at 6.8 MW). These components are integrated to work together as a single system, controlled through the microgrid controller.

The MMGS is operating mainly in a grid connected mode to achieve and maintain energy efficiency, stability, reliability, and power quality, but it can operate in an island mode during emergency cases for network security. The power generation and load of the MMGS can be controlled through the balancing of power demand and supply to achieve the PEA acceptable standards under various conditions. Fig. 1 shows the schematic diagram of the Maesariang Microgrid System. The service area of the MMGS is shown in Fig. 2.

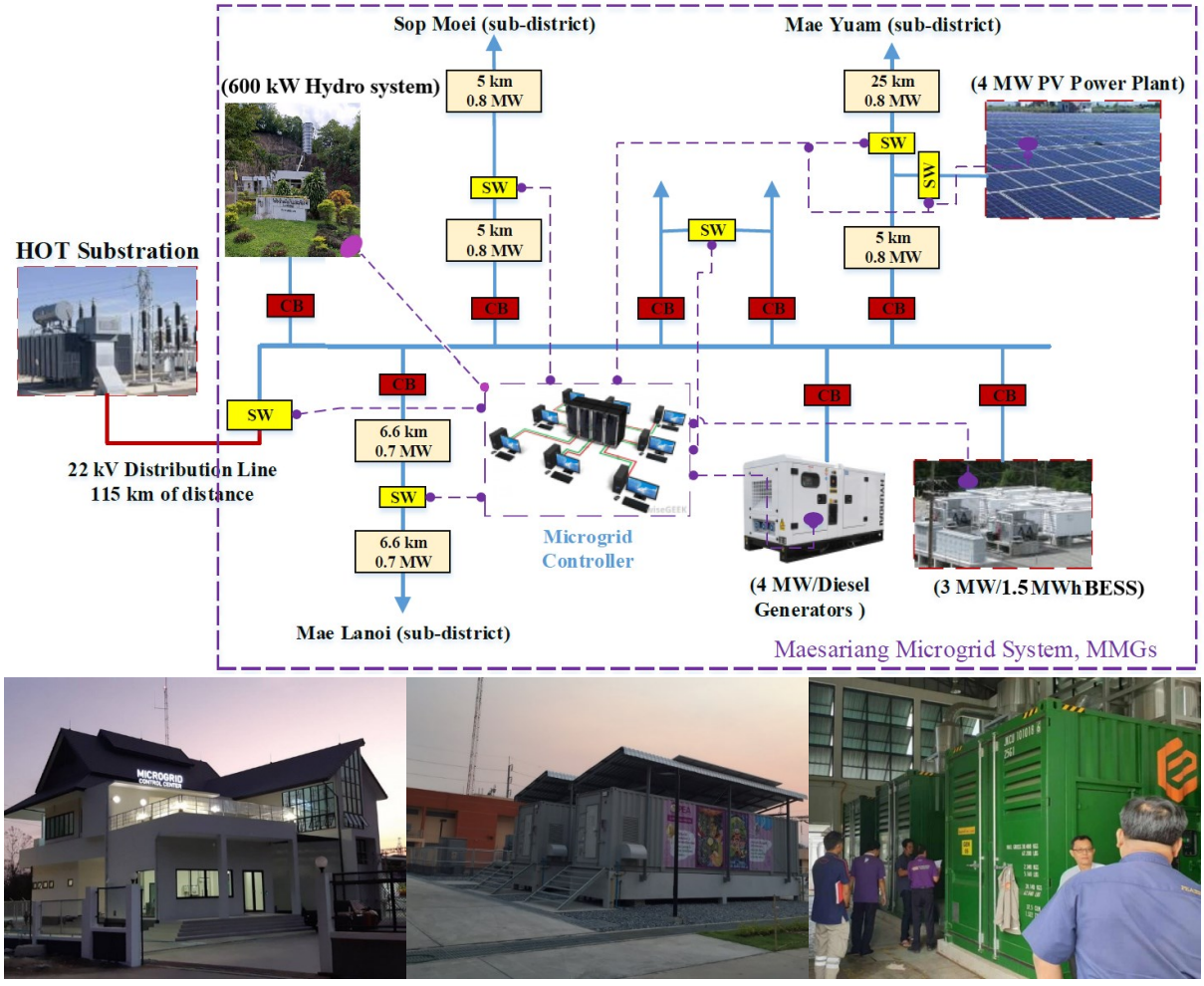

Fig. 1 Maesariang Microgrid System (MMGS).

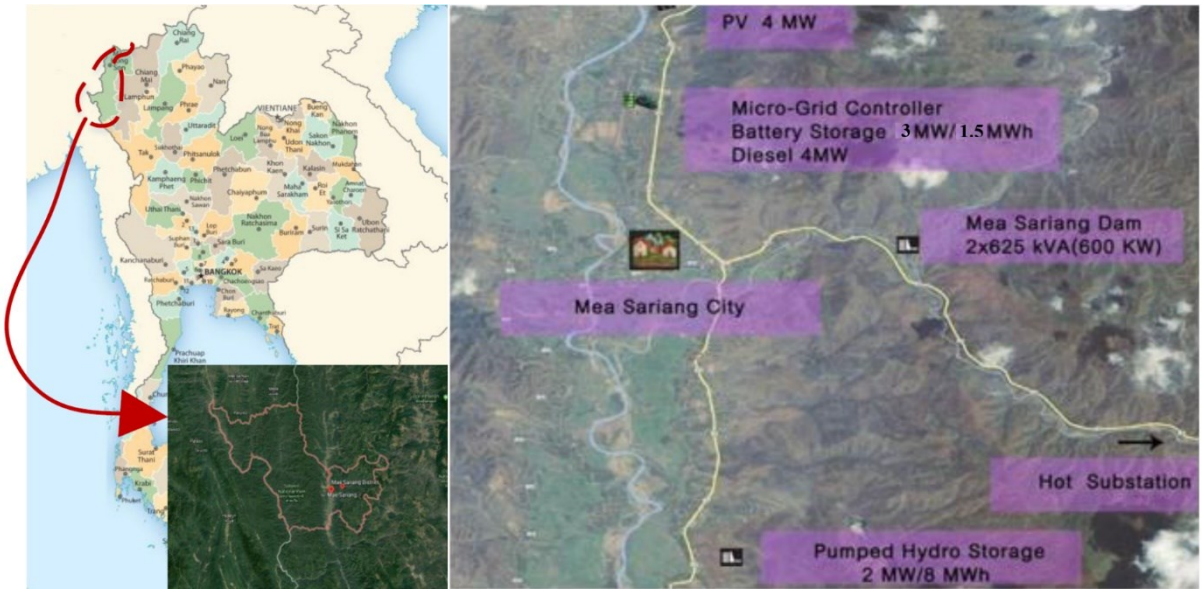

Fig. 2 The service area of MMGS.

3.2. Stability Analysis (RMS) and Electromagnetic Transient (EMT) simulation

With the DigSILENT Power Factory software, the RMS/EMT simulation that integrate a simulation scan feature and flexible co-simulation options can be used for diagnosing mid- to long-term transients under balanced or unbalanced conditions [18]. RMS/EMT simulation is used for responding to power system transient problems such as lightning, switching and temporary over-voltages, inrush currents, ferro-resonance effects or sub-synchronous resonance problems that integrate co-simulation options. It offers the greatest flexible and powerful platform for dealing with power system electromagnetic transient problems [19].

The active and reactive power flow can be calculated from equations (1) and (2). The typical bus *i* and *j* voltage of the system is presented in the polar coordinates. The final current is delivered to the network at the bus *i* in terms of the element *Yij* [20, 21]. Two-bus load flow equivalent circuit is illustrated in Fig. 3.

$$P_i = |U_i| \sum_{j=1}^{n} |U_j| \, |Y_{ij}| \cos(\theta_{ij} - \delta_i + \delta_j) \tag{1}$$

$$Q_i = |U_i| \sum_{j=1}^{n} |U_j| \, |Y_{ij}| \sin(\theta_{ij} - \delta_i + \delta_j) \tag{2}$$

where:

P = Active Power
Q = Reactive Power
U = Voltage Magnitude
I = Current
Y = Admittance
δ = Voltage angle

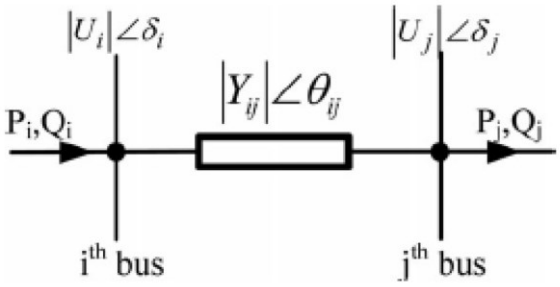

Fig. 3 Two-bus load flow equivalent circuit.

As shown on the MMGS single line diagram in Fig. 1, the PEA bus at Maesariang substation, to which the BESS and DG are connected, is regarded as the slack bus, while the 22 kV line from the Hot substation and the other buses that the HG and PV systems are connected to, are considered as the PV bus. For the other buses, they are defined as the PQ bus.

As mentioned earlier, the DigSILENT Power Factory software was used in the RMS/EMT simulation to diagnose the change of the mode of operation of the MMGS from grid connected to island mode. During the 50-second duration of the simulation, the switch that connect the MMGS with the Hot substation was opened and then closed immediately to change from a grid connected mode to an island mode, and vice versa.

The PV active power, the BESS active/reactive power, and the BESS voltage/frequency at Maesariang substation were computed as a time function of the simulation and analyzed with reference to PEA acceptable range of grid voltage and frequency (see Fig. 4). The network security, stability, reliability, and power quality of MMGS during the switching operation mode in each simulation case, with and without the communication delay effect, was studied.

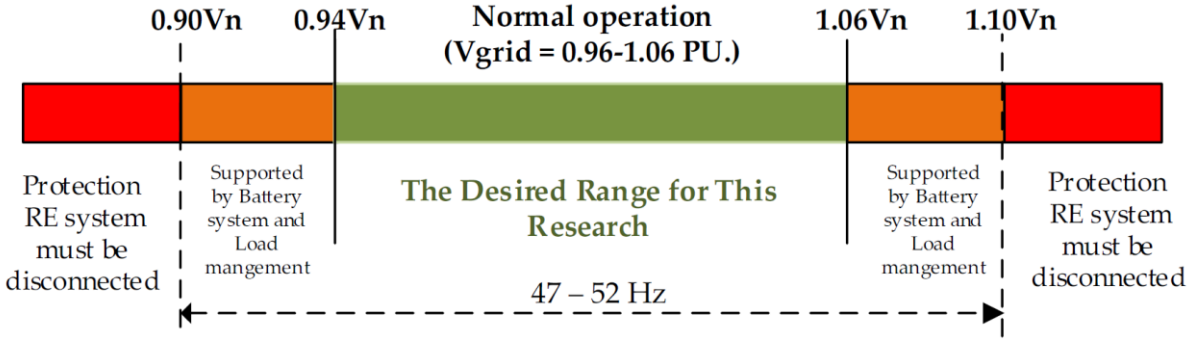

Fig. 4 PEA acceptable range of grid voltage and frequency.

3.3. Simulation Scenarios

In the operation of the MMGS, the BESS is the most important tool that can be used for maintaining the network security, stability, reliability, and power quality especially in short time periods (not over 30 minutes) because it can quickly generate or absorb power within the microgrid system for balancing the electricity generation and load, with the voltage and frequency variations maintained within the acceptable ranges of the PEA regulation. On the other hand, the power generation from the PV system can disturb the network security, stability, reliability, and power quality of the MMGS as it can rapidly fluctuate without warning because of the variation of the solar irradiance. This result to lack of control in balancing the electricity generation and load in the microgrid system, resulting to being unable to maintain the voltage and frequency within the acceptable ranges of PEA regulation.

Therefore, this simulation study focused on the active power flow behavior from the PV system and the BESS line at Maesariang substation. In addition, the response of reactive power, voltage, and

frequency from BESS line at Maesariang substation were also the focus of the simulation. For the other generators such as the DG and HG, they had minor roles in the short-term simulation because they usually generate power at constant values, and changes in their power generation rates are much slower when compared with the PV system and BESS.

There were four simulation cases or scenarios in this paper. The first two cases involved a change of the operation from a grid connected mode to an island mode; and the next two cases involved a change of the operation from an island mode to a grid connected mode. In addition, two cases analyzed the effect of connecting and disconnecting the DG to the microgrid system, after changing from a grid connected mode to an island mode.

The details of the four simulation scenarios are shown in Table 1 The simulation diagrams using the DigSILENT Power Factory software for the first to the fourth simulation cases are presented in Figs. 5 to 9, respectively.

Table 1 The details of the simulation scenarios.

Generation & load	Changing from grid connected to island		Changing from island to grid connected	
	Scenario 1	Scenario 2	Scenario 3	Scenario 4
PV system	-3.316 MW@ 10s	-3.800 MW@ 10s	-3.368 MW@ 10s	-3.380 MW@ 10s
BESS	-1.676 MW@ 10s	-0.970 MW@ 10s	-0.998 MW@ 10s	-1.200 MW@ 10s
HG	-0.400 MW@ 10s	-0.330 MW@ 10s	-0.400 MW@ 10s	-0.320 MW@ 10s
DG	-1.408 MW@ 10s	0.000 MW@ 10s -2.000 MW@ 10.2s -4.000 MW@ 10.4s	-2.534 MW@ 10s	-2.000 MW@ 10s 0.000 MW@ 13s
MMGS load without Hot substation line	6.800 MW@ 10s	6.800 MW@ 10s	6.800 MW@ 10s	6.800 MW
Hot substation line incoming	-0.500 MW@ 10s	-2.2 MW@ 10s 0.000 MW@ 10.2s	0.000 MW@ 10s	0.000 MW@ 10s
Hot substation line load in MMGS	0.500 MW@ 10s	0.500 MW@ 10s	0.500 MW@ 10s	0.500 MW@ 10s

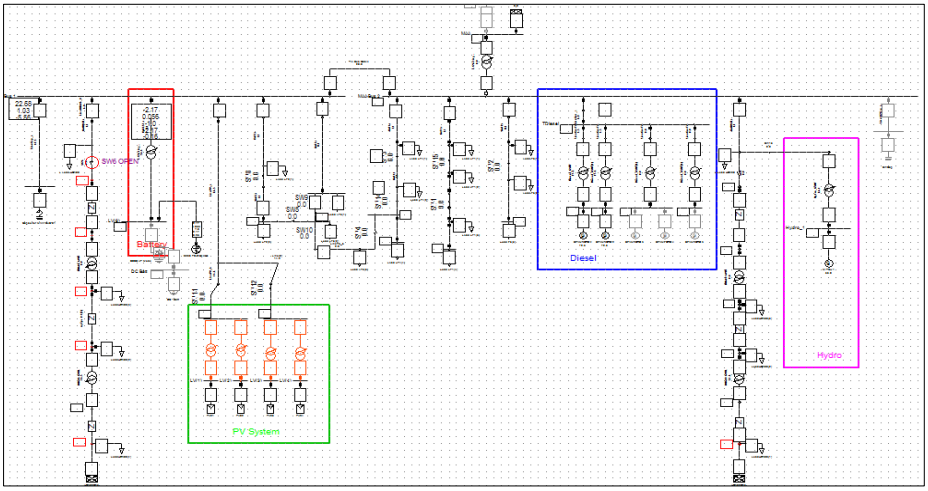

Fig. 5 The simulation diagrams in DigSILENT Power Factory software of 1st simulation case.

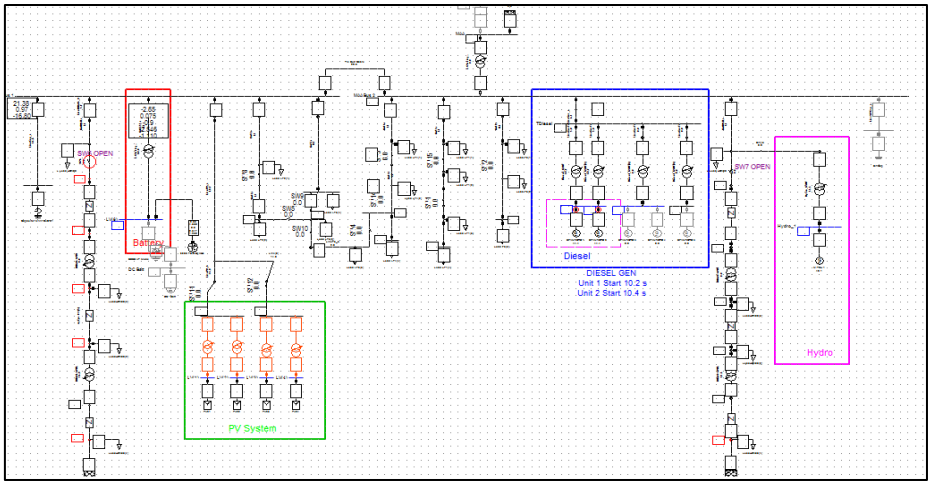

Fig. 6 The simulation diagrams in DigSILENT Power Factory software of 2nd simulation case.

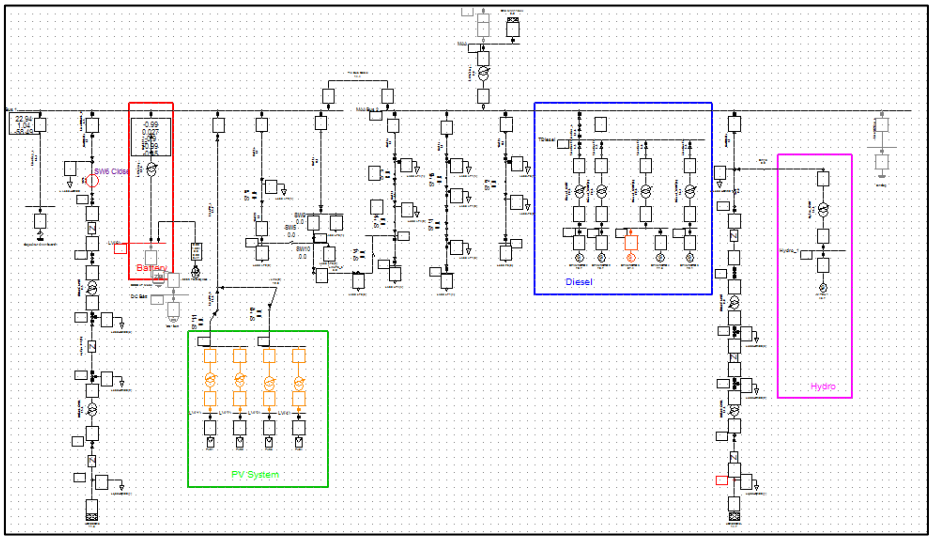

Fig 7 The simulation diagrams in DigSILENT Power Factory software of 3rd simulation case.

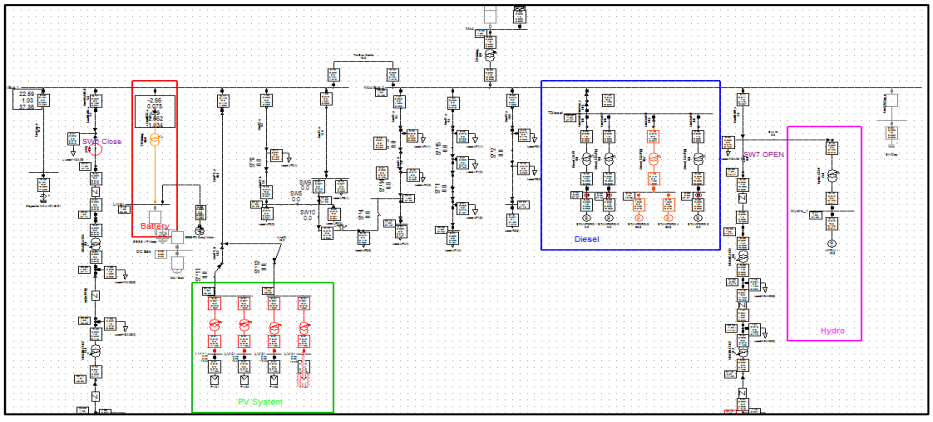

Fig. 8 The simulation diagrams in DigSILENT Power Factory software of 4th simulation case.

4. Results and Discussion

4.1. Simulation Scenario 1: *Grid Connected Mode to Island Mode Microgrid*

The electrical generation and load components of the MMGS, under simulation scenario 1, before the 10-second shifting operation of the microgrid from grid connected to island mode, are shown on Table 1. The operation diagram of the grid connected MMGS is shown on Fig. 9. Within the ten-second shifting operation, the 22 kV switch (SW6) that connected the Hot substation line with the MMGS was opened, and the MMGS was disconnected from the Hot substation, changing the operation mode of the MMGS from grid connected to island mode. The operation diagram of the MMGS in the island mode is shown in Fig. 10.

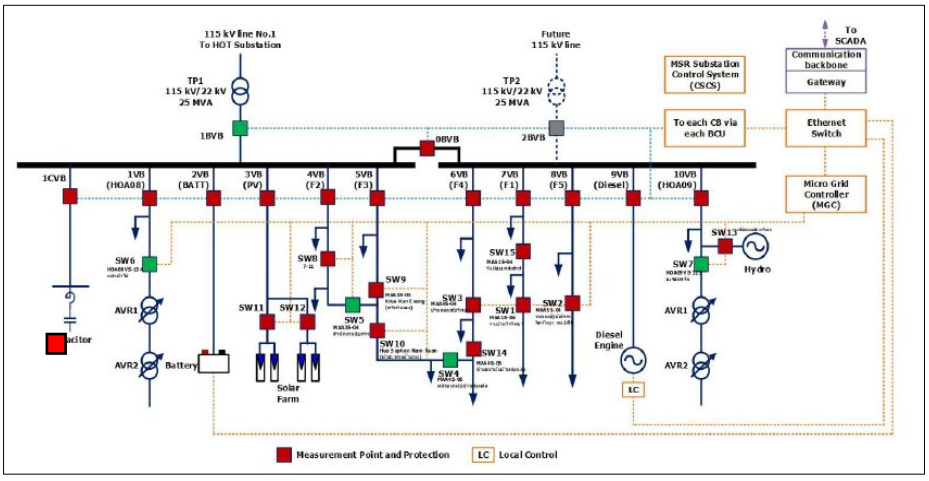

Fig. 9 The 1st case operation diagram of MMGS before switching mode from grid connected mode to island mode at 10 s.

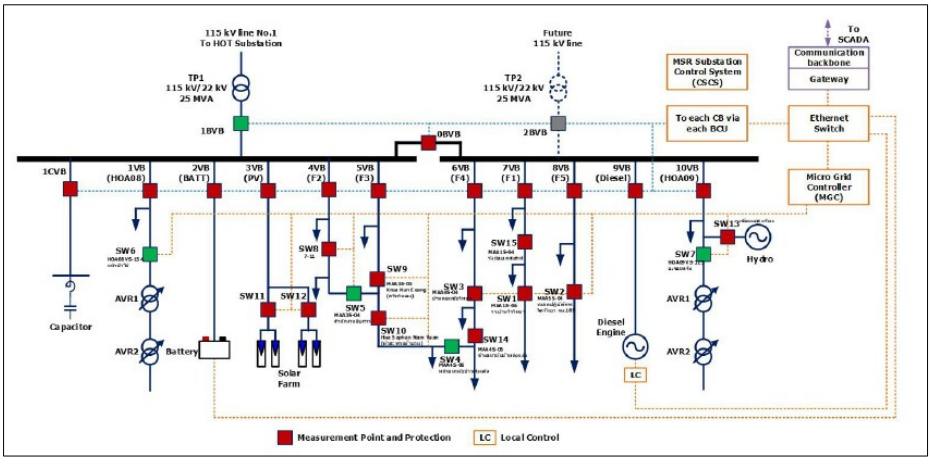

Fig. 10 The 1st case operation diagram of MMGS after switching mode from grid connected mode to island mode at 10 s.

1) "No communication time delay" Case

The behavior of the active power flow from the PV system and the BESS line, and the reactive power, voltage, and frequency response of the BESS line at Maesariang substation during the 50-second simulation period, where there was no delay in the communication time, are shown by the graphs in Fig. 11. The graphs clearly show that during the initial 10-second period, the active power generation

from the PV system was steady at 3.31 MW while the active power generation from the BESS was increasing rapidly. Moreover, the reactive power generation from the BESS was quickly dropping and then changed to absorb reactive power at a fast-increasing rate. The BESS line voltage was slightly increasing while BESS line frequency was slightly decreasing.

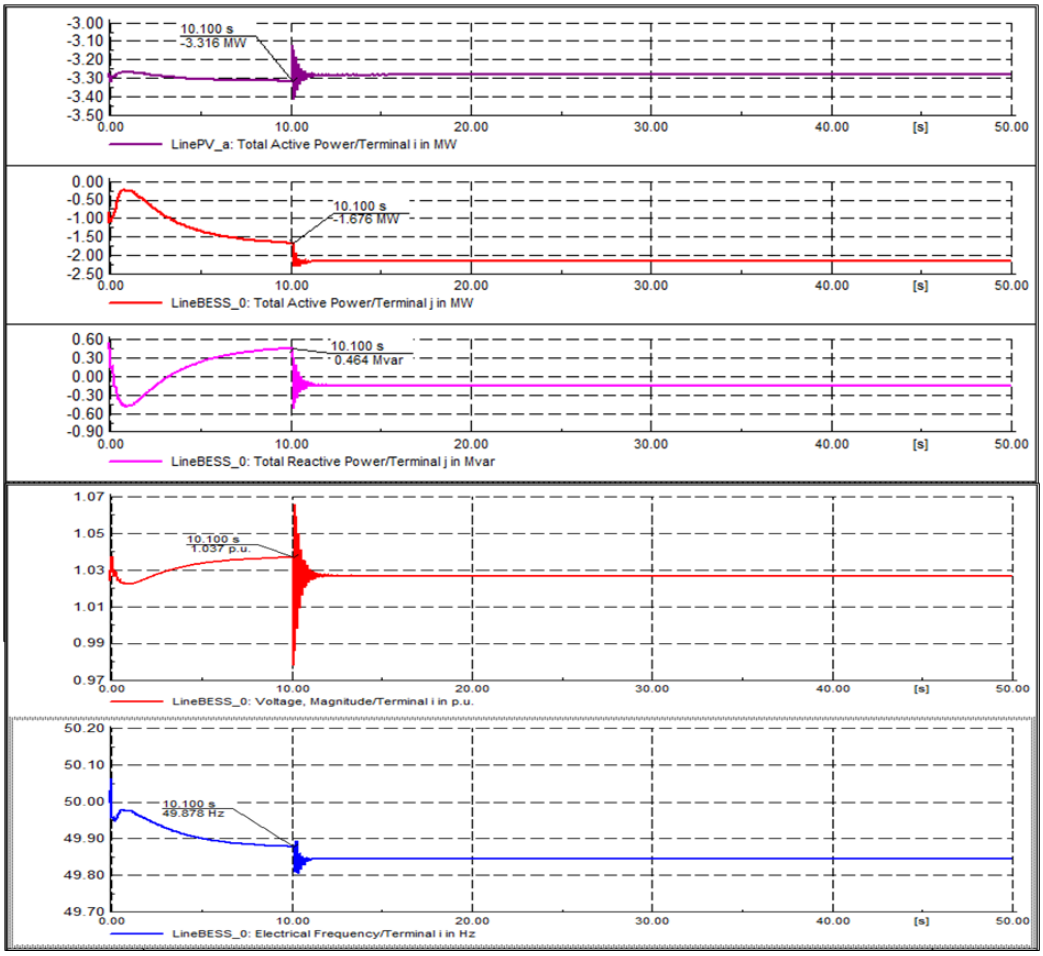

Fig. 11 The active power of the PV system and BESS line and the reactive power, voltage, and frequency of BESS line without communication time delay at Maesariang substation in 50 s of the switching mode periods.

After the 10 seconds during which the SW6 was switched off and the MMGS was disconnected from the Hot substation, the following, which can be seen correspondingly in the graphs in Fig. 11, were observed within the 50-second simulation period:

- the active power generation from the PV system fluctuated between 3.10 – 3.40 MW for one second and then stabilized at nearly 3.30 MW in ten seconds.
- the active power generation from the BESS suddenly increased to 2.25 MW slightly fluctuated for one second and stabilized at about 2.13 MW,
- the reactive power from the BESS fluctuated between 0.50 generating MVar to 0.50 absorbing MVar for one second, and stabilized at generating 0.15 MVar,
- the BESS voltage fluctuated between 0.98–1.06 p.u., then stabilized at nearly 1.03 p.u., which is in the normal range of PEA grid code, and
- the BESS frequency suddenly decreased to 49.8 Hz, slightly fluctuated for one second, and then stabilized at 49.84 Hz at 11 seconds, this is nearly the same as the rated frequency of 50 Hz.

The values of these electrical parameters during the switching of the operation mode from grid connected to island mode, and where there was no delay in the communication time (during the 10-second switching time and the rest of the 50-second simulation period), point out the excellent performance of the MMGS in controlling the network security, stability, reliability, and power quality under this 1st simulation case study.

2) "One second communication time delay" Case

The active power flow behavior from the PV system and the BESS line, and the reactive power, voltage, and frequency responses of the BESS line at Maesariang substation, with one second delay in communication time, during the 50-second simulation period, are shown correspondingly in the graphs in Fig. 12. The graphs show that the active power generation from the PV system, and the active and reactive power generation, voltage, and frequency from the BESS, have the same pattern of as in having no delay in communication, but the switching time was extended for one second.

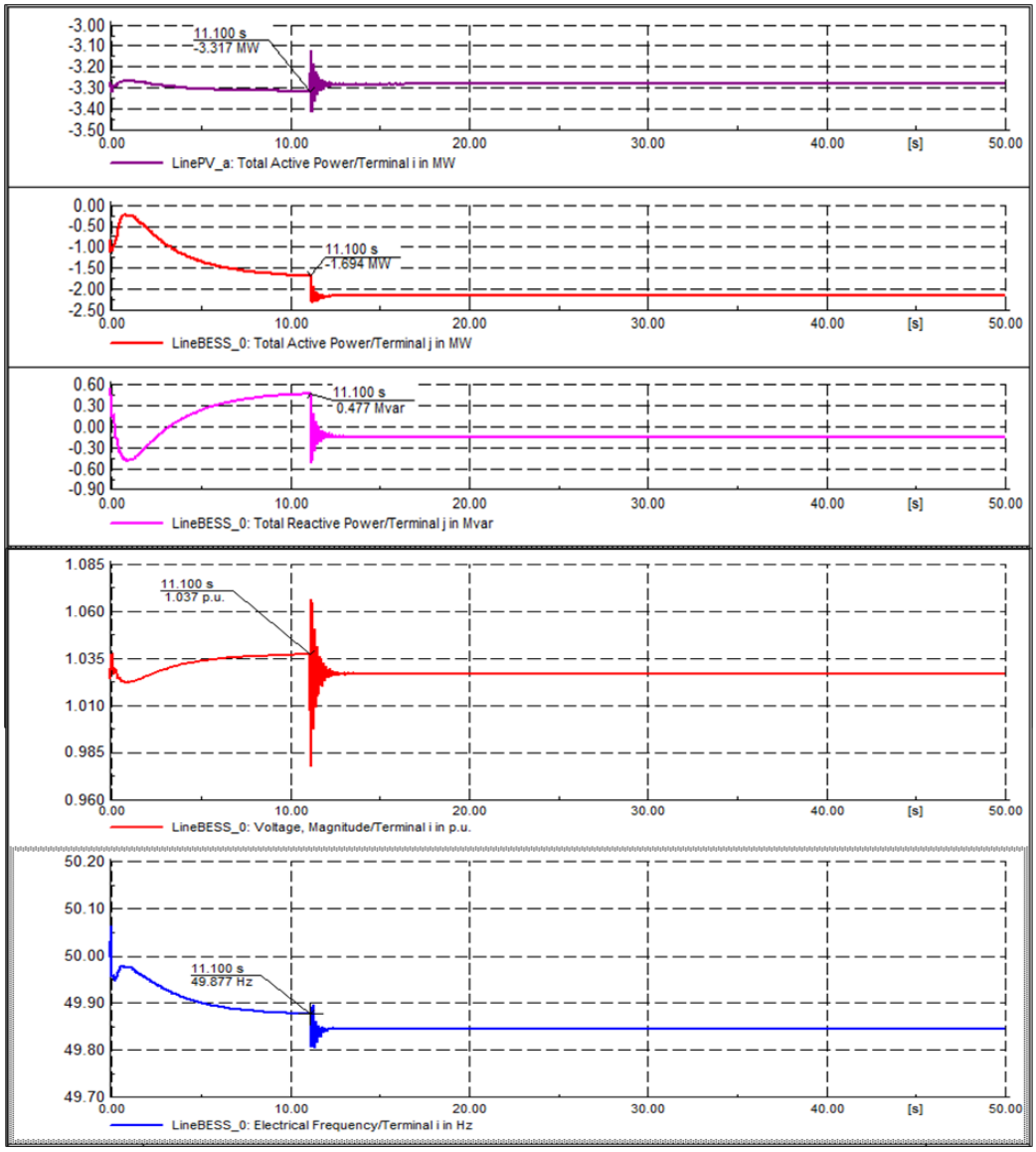

Fig.12 The active power of the PV system and BESS line and the reactive power, voltage, and frequency of BESS line with 1 s communication time delay at Maesariang substation in 50 s of the switching mode periods.

After the 11 seconds during which the SW6 was switched off and the MMGS was disconnected from Hot substation, the following, which can be correspondingly seen in the graphs in Fig. 12, were observed during the 50-second simulation period:

- the active power generation from the PV system and the active power, reactive power, voltage, and frequency from the BESS has the same pattern with no communication delay case but the time is delayed for one second.
- the electrical parameters during the 11-second shifting time from grid connected mode to island mode and during the following time of the rest of the 50-second simulation period, have the same performance as the "no communication time delay" case.

This was an indication that the "one second communication time delay" had no effect to the electrical parameters during the switching of the mode operation in this 1st simulation case.

4.2. Simulation Scenario 2: *Grid Connected Mode to Island Mode Microgrid*

The electrical generation and load components of the MMGS, under simulation scenario 2, before the 10-second shifting of the microgrid from grid connected to island mode, are shown on Table 1. The operation diagram of the grid connected MMGS is shown on Fig. 13. Within the ten-second shifting operation, the 22 kV switch (SW6) that connected the Hot substation line with the MMGS was opened, and the MMGS was disconnected from the Hot substation, changing the operation mode of the MMGS from grid connected to island mode. The operation diagram of the MMGS in the island mode is shown in Fig.14.

1) "No communication time delay" Case

The behavior of the active power flow from the PV system and BESS line, and the reactive power, voltage, and frequency response of the BESS line at Maesariang substation during the 50-second simulation period, where there was no delay in the communication time, are shown by the graphs in Fig. 15. The graphs clearly show that during the initial ten seconds, the active power generation from the PV system was steady at 3.80 MW while the active power generation from the BESS increased to 1.00 MW. Moreover, the reactive power generation from the BESS decreased to 1.00 MVar. The BESS line was steady at 1.04 p.u., and so was the BESS line frequency, which was also steady at 50 Hz.

After the ten seconds during which the SW6 was turned off and the MMGS was disconnected from the Hot substation, the following, which can be seen correspondingly in the graphs in Fig. 15, were observed during the 50-second simulation period:

- the active power generation from the PV system immediately dropped to 1.50 MW after this and then increased again and stabilized at around 3.60 MW in 20 seconds.
- the active power generation from BESS suddenly increased to 2.60 MW and then decreased to zero within 5 seconds, it stabilized to around 2.60 MW in 22 seconds.
- the reactive power from the BESS immediately dropped to zero but increased to 1.75 MVar within 5 seconds, it then stabilized to around 1.20 MVar in 23 seconds.
- the BESS voltage decreased to 0.45 p.u. in five seconds, and then increased before it stabilized to around 0.98 p.u. within 22 seconds; this was out of the normal range of PEA grid code.
- the BESS frequency decreased to 47.50 Hz, then increased again to 50 Hz, and then lightly dropped again stabilized at 49.80 Hz, all of these in 20 seconds; this is nearly out of the frequency range in PEA grid code.

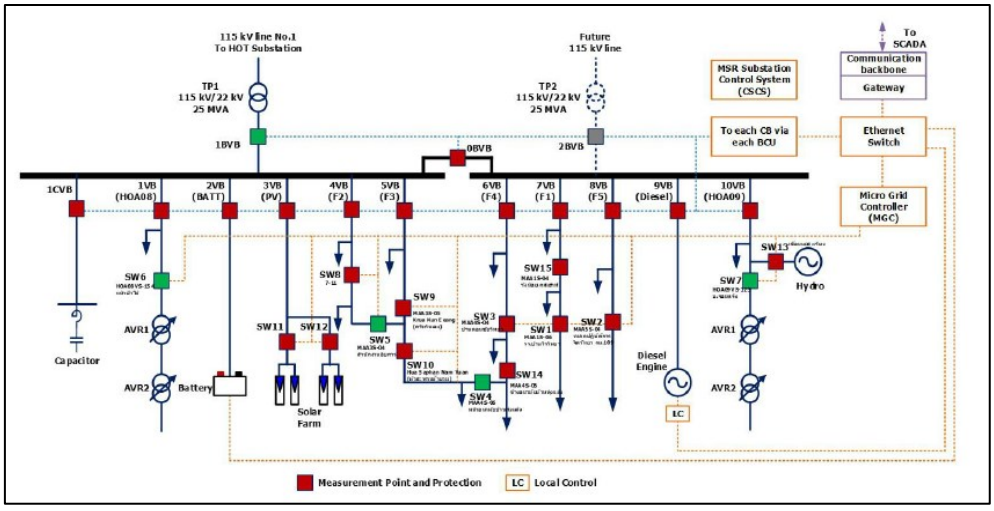

Fig. 13 The 2nd case operation diagram of MMGS before switching mode from grid connected mode to island mode at 10 s.

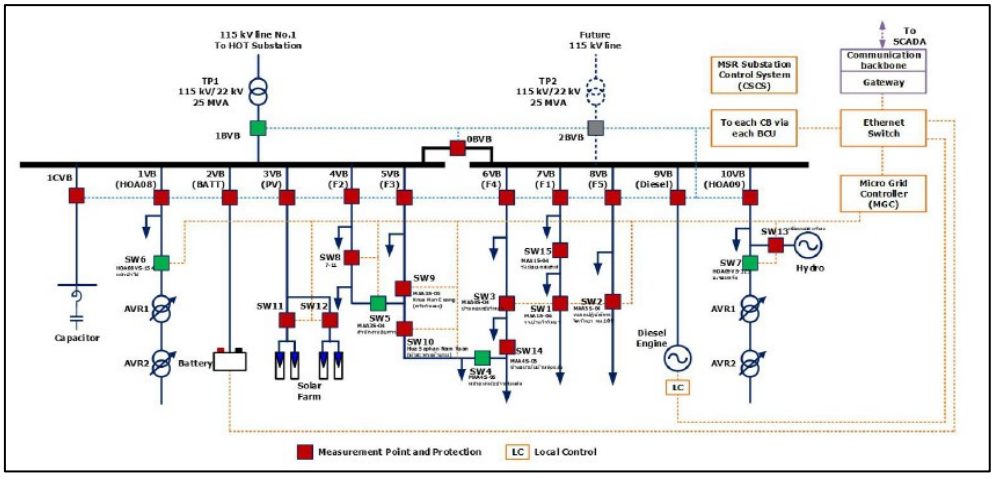

Fig. 14 The 2nd case operation diagram of MMGS after switching mode from grid connected mode to island mode at 10 s.

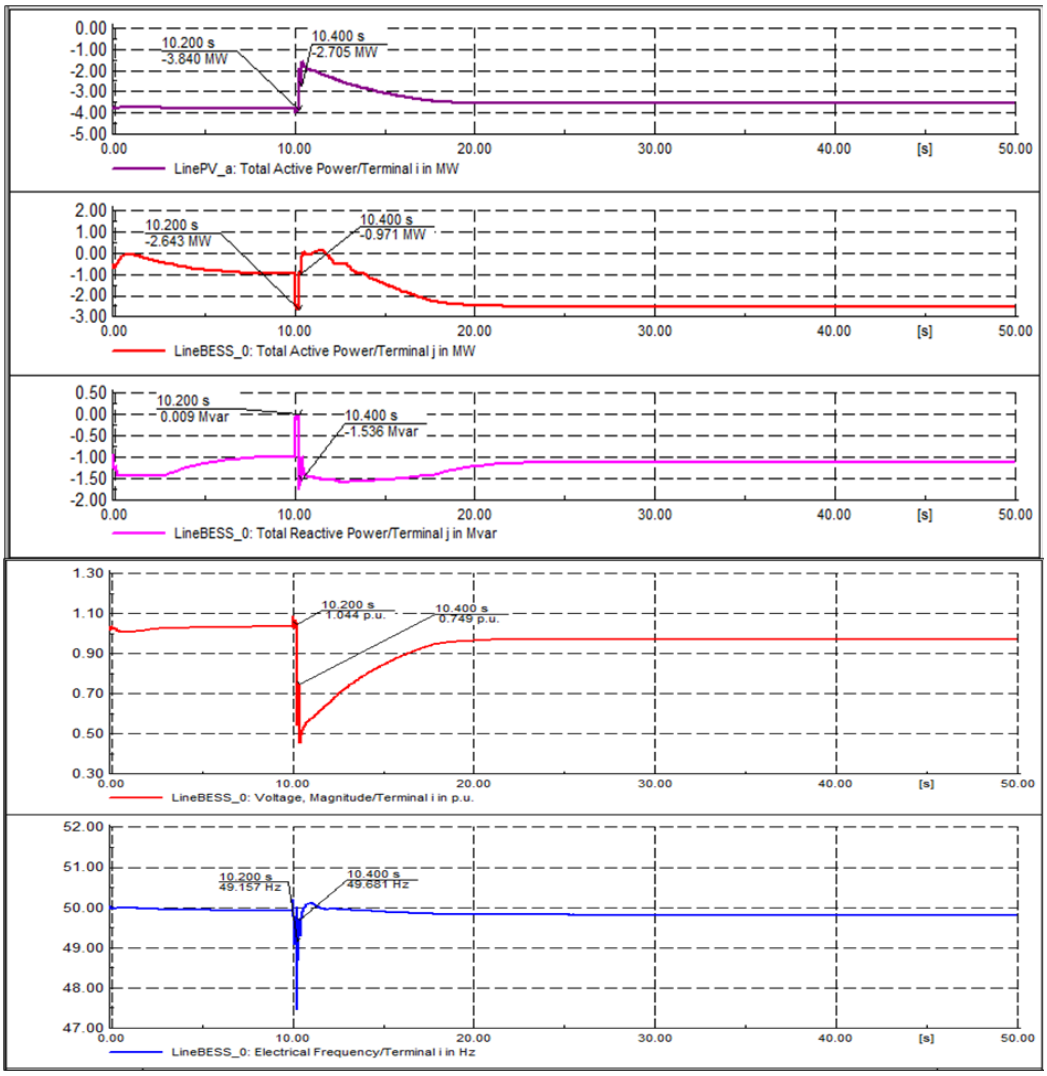

Fig. 15 The active power of the PV system and BESS line and the reactive power, voltage, and frequency of BESS line without communication time delay at Maesariang substation in 50 s of the switching mode periods.

The values of these electrical parameters during the switching of the operation mode from grid connected to island mode and where there was no delay in the communication time (during the 10-second switching time and the rest of the 50-second simulation period), indicate a moderate performance of the MMGS in controlling the network security, stability, reliability, and power quality under this 2nd scenario simulation case.

2) "One second communication time delay" Case

If there was one second delay in communication time, this could not be simulated, because the DG could not start in time, and this could have resulted to system failure and blackout in the MMGS. This showed the poor performance of the MMGS in controlling the network security, stability, reliability, and power quality during mode switching under the 2nd scenario simulation case, where there is one-second delay in communication time. The communication time delay is a key factor to protect the MMGS from blackouts during the shifting of the grid operation mode under the 2nd scenario simulation case.

4.3. Simulation Scenario 3: *Island Mode to Grid Connected Mode Microgrid*

The electrical generation and load components of the MMGS, under simulation scenario 3, before the 10-second shifting of the microgrid from island to grid connected mode, are shown on Table 1. The operation diagram of the MMGS island mode is shown on Fig. 16. Within the ten-second shifting operation, the 22 kV switch *(*SW6*)* that connected the Hot substation line with the MMGS was closed, and the MMGS was connected from the Hot substation, changing the operation mode of the MMGS from island to grid connected mode. The operation diagram of the grid connected MMGS is shown in Fig. 17.

1) "No communication time delay" Case

The behavior of the active power flow from the PV system and the BESS line, and the reactive power, voltage, and frequency response of the BESS line at Maesariang substation during the 50-second simulation period, where there was no communication time delay, are shown by the graphs in Fig. 18. The graphs show that within the first 10 second period, the active power generation (at 2.37 MW) from the PV system, and the active power generation (1.00 MW), reactive power generation (0.38 MVar), voltage (1.04 p.u.), and frequency (49.92 Hz) of the BESS, were all steady.

After the ten seconds during which the SW6 was closed and the MMGS was connected to the Hot substation, the following, as can be seen correspondingly in the graphs in Fig. 18, were observed:

- the active power generation from the PV system fluctuated between 2.20 - 2.41 MW for two seconds, and then stabilized to around 2.36 MW within 20 seconds.
- the active power generation from the BESS suddenly increased to 3 MW and then decreased and changed to absorption power to about 2.10 MW in 2 seconds, the active power absorption continued to decrease until it changed to power generation and stabilized at 1.00 MW within 20 seconds.
- the reactive power from the BESS immediately changed from generation to absorption to about 0.50 MVar in 10 seconds, and then switched back to generation to about 1.80 MVar before stabilizing to around 0.40 MVar in 28 seconds.
- the BESS voltage was fluctuating between 1.060 - 0.985 p.u. for two seconds, and then increased slightly and stabilized to around 1.045 p.u. within 24 seconds, this was within in the normal range of the PEA grid code.
- the BESS frequency was swinging between 49.50 to 50.20 Hz for 2 seconds, and then, dropped lightly and stabilized to 49.92 Hz within 26 seconds, this was near the rated frequency value.

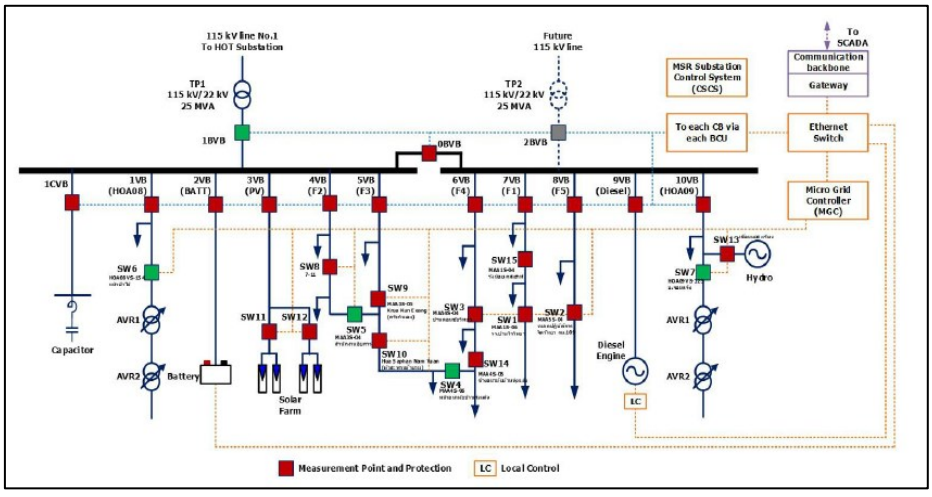

Fig. 16 The 3rd case operation diagram of MMGS before switching mode from island mode to grid connected mode at 10 s.

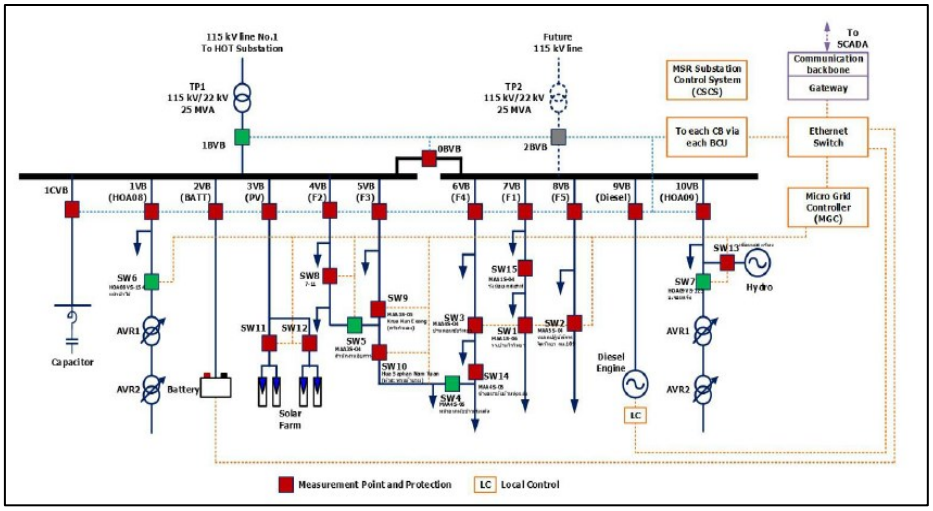

Fig. 17 The 3rd case operation diagram of MMGS after switching mode from island mode to grid connected mode at 10 s.

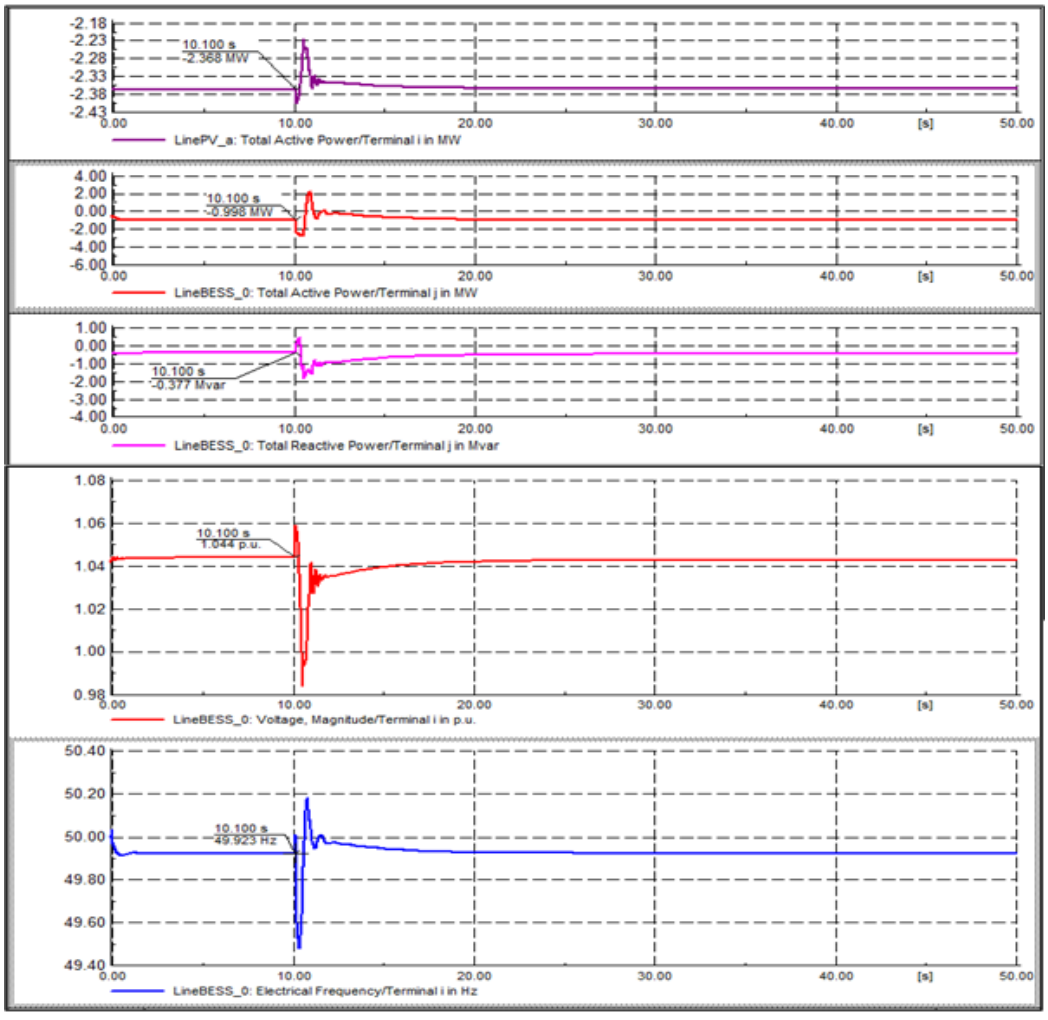

Fig. 18 The active power of the PV system and BESS line and the reactive power, voltage, and frequency of BESS line without communication time delay at Maesariang substation in 50 s of the switching mode periods.

In this 3rd simulation case, the change in the operation mode from island to grid connected mode was for 10 seconds and there was no communication time delay. The values for the electrical parameters during the change in the operation mode from island to grid connected mode showed the excellent performance of the MMGS in controlling the network security, stability, reliability, and power quality.

2) "One second communication time delay" Case

The behavior of the active power flow from the PV system and the BESS line, and the response reactive power, voltage, and frequency of the BESS line at the Maesariang substation, in the case where there is one second delay in communication time during the 50-second simulation period, are shown by the graphs in Fig. 19. The graphs show that the active power generation from the PV system, and the active and reactive power generation, voltage, and frequency from the BESS, wherein the operation mode shifting time was extended for one second, have all the same pattern as with the case where there was no delay in communication time.

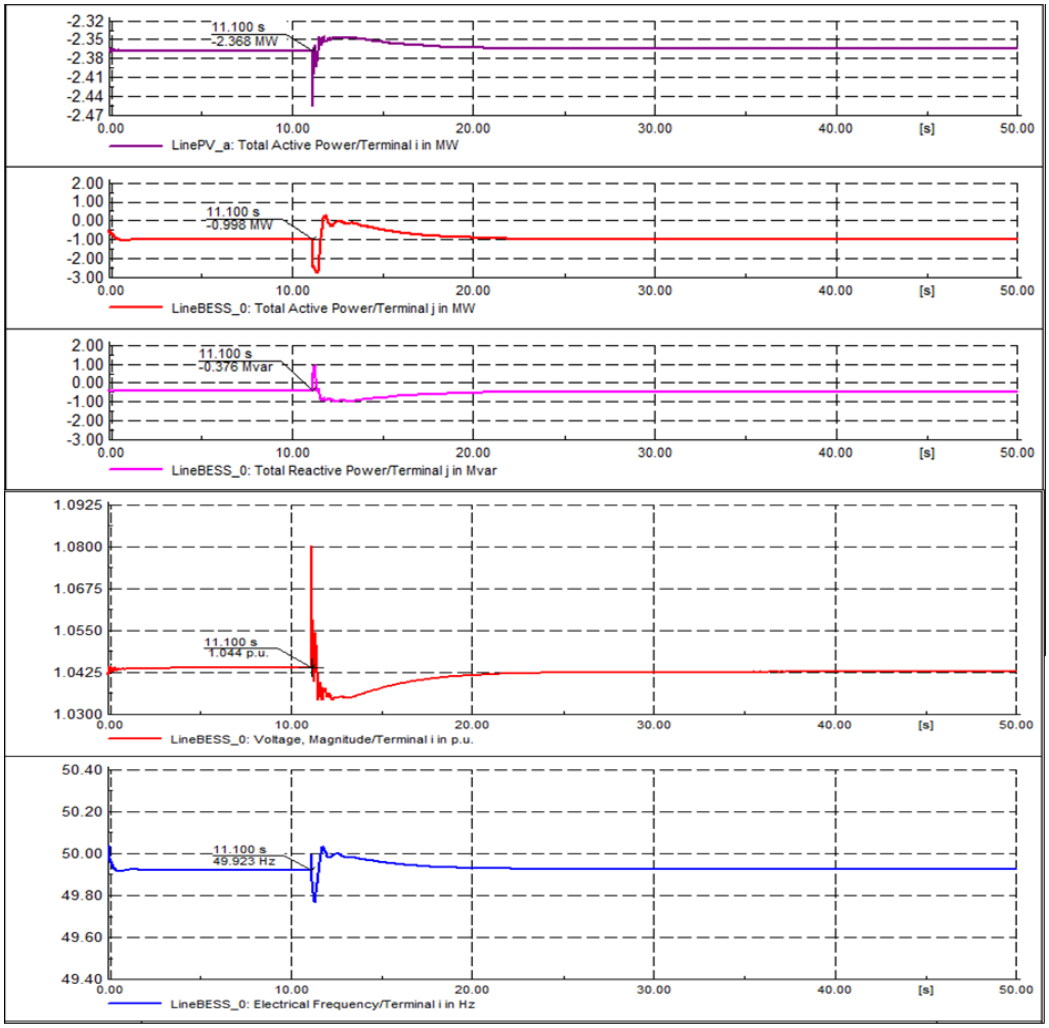

Fig. 19 The active power of the PV system and BESS line and the reactive power, voltage, and frequency of BESS line with 1 s communication time delay at Maesariang substation in 50 s of the switching mode periods.

After the 11 seconds during which the SW6 was closed and the MMGS was connected to the Hot substation, the following, as can be seen correspondingly in the graphs in Fig. 19, were observed:

- the active power generation from the PV system immediately increased to 2.46 MW, then dropped and stabilized to around 2.36 MW within 22 seconds.
- the active power generation from the BESS was swinging from zero to 2.75 MW, and then stabilized at 1 MW within 23 seconds.
- the reactive power from BESS was swinging from 1.00 MVar generation to 1.00 MVar absorption for two seconds, before stabilizing at around 0.4 MVar in 22 seconds.
- the BESS voltage was oscillating between 1.035 p.u. to 1.080 range for 2 seconds, it slightly increased and then stabilized down to around 1.043 p.u. in 24 seconds, this was over the normal range of PEA grid code by about 0.1 second.
- the BESS frequency was fluctuating between 49.75 to 50.05 Hz for 2 seconds, it slowly decreased and then stabilized at 49.92 Hz within 23 seconds, which was near the rated frequency.

The values of these electrical parameters during the switching from island mode to grid connected mode where there was no delay in the communication time (during the 11-second switching time and the rest of the 50-second simulation period) have nearly the same performance with the case where there is no communication time delay. It showed that the one second communication time delay had scanty effect on the electrical parameters during switching of the microgrid operation mode in the 3rd simulation case.

4.4. Simulation Scenario 4: *Island Mode to Grid Connected Mode Microgrid*

Under the 4th simulation scenario, the generation and load components of the MMGS before the change in the mode of operation from island to grid connected mode is shown on Table 1. The operation diagram of the MMGS in island mode is shown on Fig. 20. Within 10 seconds, the SW6 that connected the Hot substation line with the MMGS was closed, the MMGS was connected to the Hot substation, and the MMGS switched from an island to a grid connected mode of operation. The operation diagram of the grid connected MMGS is shown in Fig. 21.

1) "No communication time delay" Case

The behavior of the active power flow from the PV system and the BESS line, and the reactive power, voltage, and frequency response of the BESS line at the Maesariang substation, for which there was no communication time delay, during the 50-second simulation period, are shown by the graphs in Fig. 22. The graphs show that from zero to ten seconds, the active power generation from the PV system and the BESS were slowly expanding to 3.40 MW and 1.20 MW, respectively. The reactive power generation of BESS was slowly decreasing to 1.00 MVar, the voltage was slightly rising to 1.08 p.u., and the frequency steady at 50 Hz.

After the 10 seconds during which the SW6 was closed and the MMGS was connected to the Hot substation, the following, as can be seen correspondingly in the graphs in Fig. 19, were observed:

- the active power generation from the PV system then swung between 2.15 MW to 3.40 MW for one second, and then stabilized to around 2.30 MW in two seconds.
- the active power from the BESS fluctuated between 2.8 MW generation to 2.40 MW absorption for two seconds, and then stabilized to around 2.8 MW generation within 2.5 seconds.
- the reactive power from BESS oscillated from 2.2 MVar generation to 1.1 MVar absorption for two seconds and stabilized around 1.55 MVar generation within 2.5 seconds.
- the BESS voltage swung between 0.72 p.u. and 1.08 p.u. for 1.5 second, and then stabilized to around 1.045 p.u. in three seconds, this was out of the voltage range of the PEA grid code.
- the BESS frequency was swinging between 48.5Hz - 50.5 Hz for two seconds, and then stabilized in 2.5 seconds at 50.0 Hz, which is the rated frequency.

The DG was disconnected from the MMGS within 13 seconds, and then the following were observed:

- the active power generation from the PV system fell suddenly to about 3.00 MW, but slowly increased and then stabilized at 3.17 MW within 25 seconds.
- the active power generation from the BESS increased slowly and stabilized at 2.80 MW in 24 seconds.
- the reactive power generation from BESS decreased slowly and stabilized at 1.20 MVar in 27 seconds.
- the BESS voltage decreased to about 0.96 p.u. and then increased and stabilized at 1.03 p.u. in 26 seconds.
- the BESS frequency slightly decreased and then stabilized at 49.80 Hz in 24 seconds.

The values of these electrical parameters during the switching of the mode of microgrid operation from an island to a grid connected mode, where there was no communication time delay time (during the 10-second switching time and the rest of the 50-second simulation period) showed an acceptable performance of MMGS in controlling the network security, stability, reliability, and power quality, under this case of the 4th simulation scenario.

The disconnection of the DG from MMGS had an insignificant effect to the electrical parameters of MMGS.

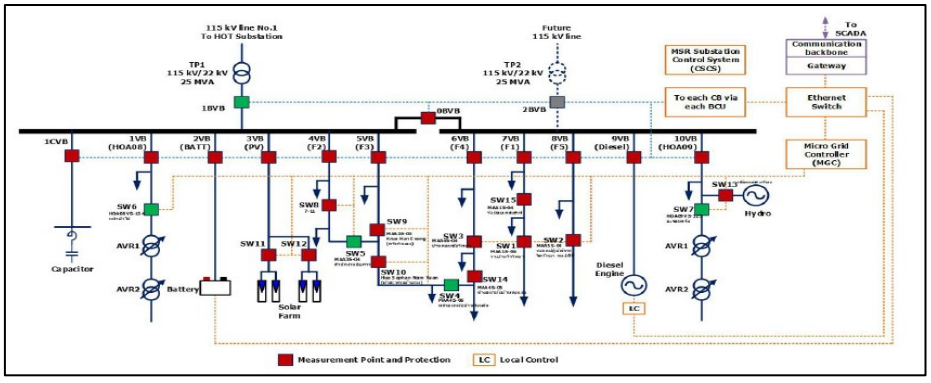

Fig. 20 The 4th case operation diagram of MMGS before switching mode from island mode to grid connected mode at 10 s.

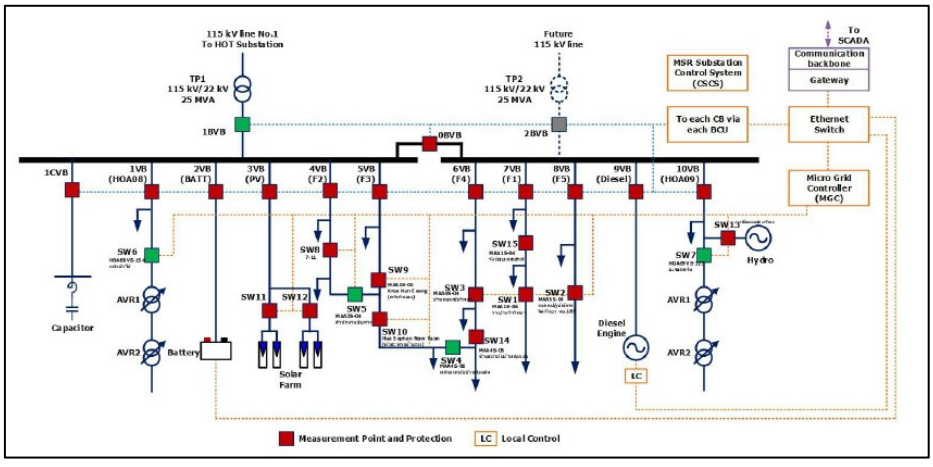

Fig. 21 The 4th case operation diagram of MMGS after switching mode from island mode to grid connected mode at 10 s.

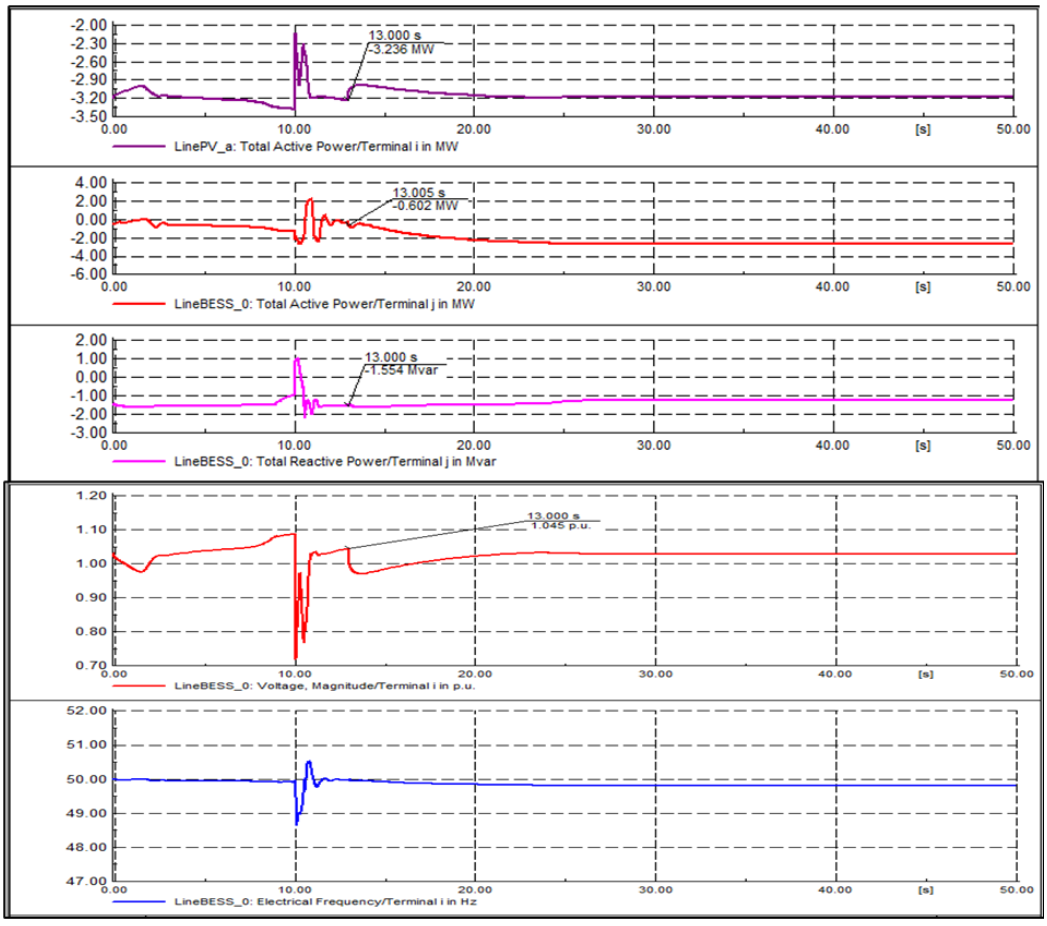

Fig. 22 The active power of the PV system and BESS line and the reactive power, voltage, and frequency of BESS line without communication time delay at Maesariang substation in 50 s of the switching mode periods.

2) "One second communication time delay" Case

The behavior of the active power flow from the PV system and the BESS line, and the response reactive power, voltage, and frequency of the BESS line at the Maesariang substation, for the case of one second communication time delay, within the 50 second simulation period, is shown by the graphs in Fig. 23. The graphs show that the active power generation from the PV system, the active and reactive power generation, voltage, and frequency from the BESS have the same pattern, as with the case with no communication time delay. However, the stabilizing time before the DG was disconnected was extended for one second. These electrical parameters during the switching from island mode to grid connected mode (during the 10-second switching time and the rest of the 50-second simulation period), have nearly the same performance as the case for no communication time delay. It showed that a one second delay in communication time has no effect on the electrical parameters during the switching of the mode operation under this case of the 4th simulation scenario.

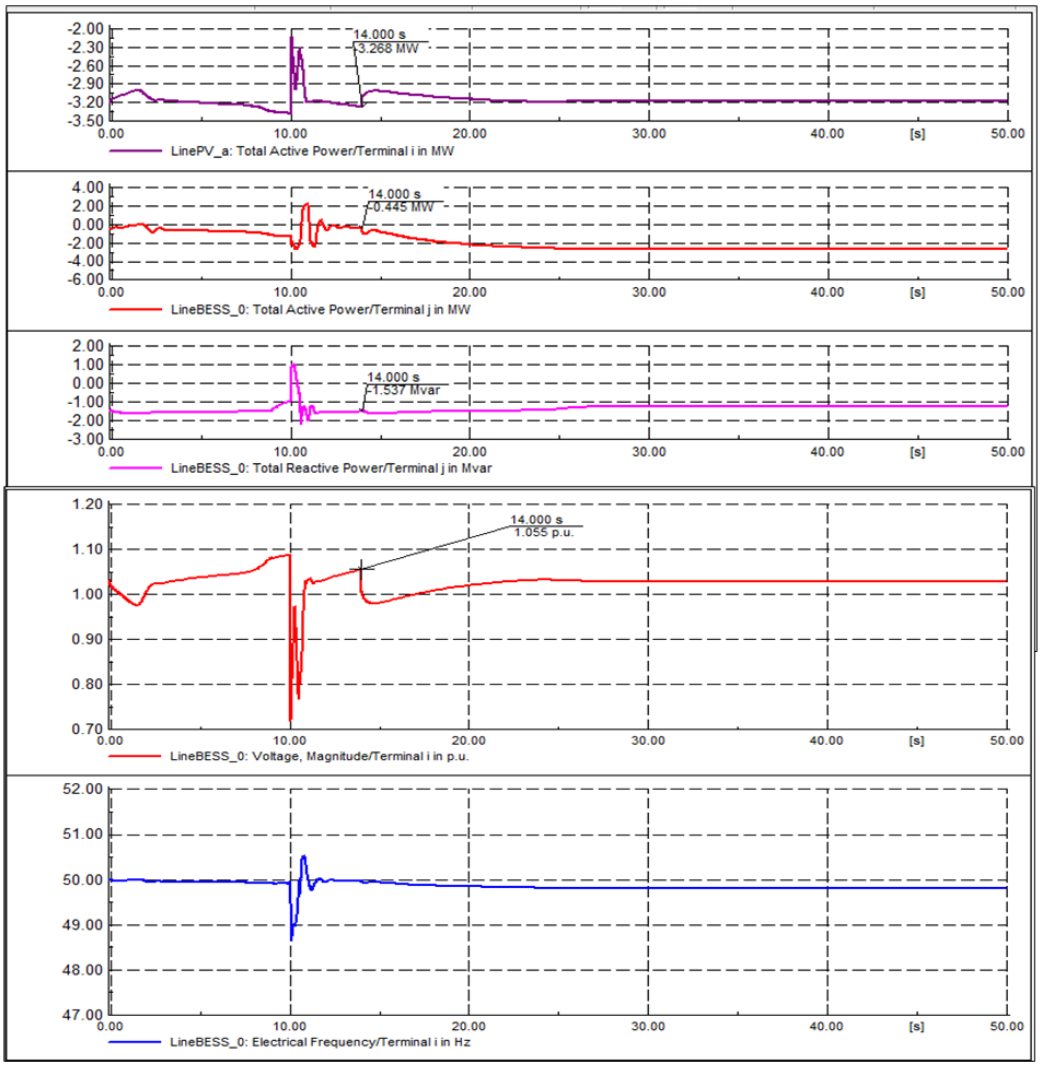

Fig. 23 The active power of the PV system and BESS line and the reactive power, voltage, and frequency of BESS line with 1 s communication time delay at Maesariang substation in 50 s of the switching mode periods.

5. Conclusions

PEA implemented the MMGS to correct the high transmission line losses, over voltage, voltage sag, and interruption problems, and to improve the network security, stability, reliability, and power quality in the Maesariang district, Mae Hong Sorn province. The district is one of the weakest power network areas under PEA service. The period for switching between a grid connected mode and an island mode is very risky for controlling the network security, stability, reliability, and power quality in the covered area. In this study, the application of the RMS/EMT simulation using the DigSILENT Power Factory software provided a powerful tool for evaluating the MMGS performance during switching operation. Four simulation scenarios were studied.

The first two simulation scenarios (the 1st and 2nd simulation scenarios) involved the shift of the operation mode of the MMGS from grid connected to island mode. The simulations studies demonstrated that the MMGS can control very well all the electrical parameters within the range of PEA grid code, and communication time delays have no effect on the performance during switching of the mode of operation from grid connected to island mode, when the spare power generation from the BESS is higher than the loses from the Hot substation line after the mode of operation have changed. In contrast, the

MMGS performed poorly in controlling all electrical parameters within the operation range of PEA grid code, when the spare generation power of BESS is equal or lower than the loses from Hot substation line after switching of the operation mode, and communication time delay is a crucial factor to prevent the blackout in MMGS during the changing of the operation mode from grid connected to island mode.

The last two simulation scenarios (the 3rd and 4th simulation scenarios) involved the shift of the operation mode of the MMGS from island to grid connected mode. These simulations demonstrated that the MMGS performed very well in controlling the electrical parameters within the operation range of PEA grid code, and that communication time delay has very small effect on the performance during shifting of the mode operation from island to grid connected mode. Only the BESS voltage, in the 4th simulation scenario, was out of the operation range of PEA grid code, but only for a noticeably short time. The disconnection of the DG from MMGS after switching the mode of operation from island to grid connected mode had negligible effect to the electrical parameters of MMGS.

The results of these simulation scenario study can possibly be used as guideline for the operation and management of the Maesariang Microgrid System in the future.

Acknowledgements

The authors wish to thank Mr. Peter Barton of the writing clinic, division of international affairs and language development **(**DIALD**)** for his help in editing English in this article. Finally, the authors would like to thank the Smart Energy System Integration Research Unit staff for their supporting information**.**

References

[1] Electricity Generating Authority of Thailand (EGAT). (1970-2019). *The peak power demand of Thailand*. Retrieved December 28, 2020, from https://www.egat.co.th/index.php?option=com_content&view=article&id=353&Itemid=200

[2] Masson, G. & Kaizuka, I. (2020). *Trends 2020 in Photovoltaic Applications*. Genval, Belgium: IEA-PVPS T1.

[3] Energy Regulatory Commission (ERC). (2018). *Summary purchase status of power plant.* Retrieved December 28, 2018, from http://www.erc.or.th/ERCSPP/default.aspx?x=0&muid=23&prid=41

[4] Panwar, L. K., Reddy, S., Verma, A., & Panigrahi, B. K. (2017). Dynamic incentive framework for demand response in distribution system using moving time horizon control. *IET Generation, Transmission & Distribution, 11*(17), 4338-4347.

[5] Arun, S. L., & Selvan, M. P. (2017). Dynamic demand response in smart buildings using an intelligent residential load management system. *IET Generation, Transmission & Distribution, 11*(17), 4348-4357.

[6] Wang, X., El-Farra, N. H., & Palazoglu, A. (2017). Optimal scheduling of demand responsive industrial production with hybrid renewable energy systems. *Renewable Energy, 100,* 53-64.

[7] Schultis, D. L. (2019). Comparison of local volt/var control strategies for PV hosting capacity enhancement of low voltage feeders. *Energies, 12*(8), 1560-1586.

[8] Aziz, T., & Ketjoy, N. (2017). Enhancing PV penetration in LV networks using reactive power control and on load tap changer with existing transformers. *IEEE Access, 18*(6), 2683-2691.

[9] Sultan, H. M., Diab, A. A., Kuznetsov, O. N., Ali, Z. M., & Abdalla, O. (2019). Evaluation of the impact of high penetration levels of PV power plants on the capacity, frequency and voltage stability of Egypt's unified grid. *Energies, 12*(3), 552-573.

[10] Chimtavee, A., Ketjoy, N., Sriprapha, K., & Vaivudha, S. (2011). Evaluation of PV Generator Performance and Energy Supplied Fraction of the 120 kWp PV Microgrid System in Thailand. *Energy Procedia, 9,* 117-127.

[11] Chimtavee, A., & Ketjoy, N. (2012). PV generator performance evaluation and load analysis of the PV microgrid system in Thailand. *Procedia Engineering, 32,* 384-391.

[12] Solaphom, K., Premrudeepreechacharn, S., Kasirawat, T., Sorndit, C., Meenual, T., & Higuchi K. (2020). Operation strategy of microgrid for rural area of northern Thailand. *International Journal of Smart Grid and Clean Energy, 9*(1), 126-134.
[13] Netisak, W. & Ketjoy, N. (2015). Agent based energy management system for microgrid. *International Journal of Renewable Energy, 10*(2), 55-62.
[14] Tonsing, M., & Setthapun, W. (2019). Big data collection procedure for on-site monitoring system of smart community with PV microgrid. *Journal of Renewable Energy and Smart Grid Technology, 14,* 87-101.
[15] Mohapatra, D., Jaeger, J., & Wiemann, M. (2019). *Private sector driven business models clean energy mini-grids: Lesson learnt from South and South-East Asia.* Brussels, Belgium: Alliance for Rural Electrification (ARE).
[16] Andrew, B. (2019). *Thailand Petroleum Co. Tests Commercial Microgrid with Blockchain for Mall and Fuel Station.* Retrieved December 28, 2020, from https://microgridknowledge.com/commercial-microgrid-blockchain-thailand/
[17] Energy Policy and Planning office (EPPO). (2018). *Prototype microgrid*. Retrieved December 28, 2020, from http://www.eppo.go.th/index.php/th/eppo-intranet/item/13654-news-19062561
[18] DigSILENT GmbH. *Stability Analysis Functions (RMS).* Retrieved December 28, 2020, from https://www.DigSILENT.de/en/stability-analysis.html
[19] DigSILENT GmbH. *Electromagnetic Transient (EMT).* Retrieved December 28, 2020, from https://www.DigSILENT.de/en/electromagnetic-transients-emt.html
[20] John, J. G. (1994). *Power system analysis.* New York, USA: McGraw-Hill.
[21] Saadet, H. (1999). *Power system analysis.* New York, USA: McGraw-Hill.